Bioorganic Chemistry 108 (2021) 104653

Contents lists available at ScienceDirect

Bioorganic Chemistry

journal homepage: www.elsevier.com/locate/bioorg

Synthesis of novel sulfonamide derivatives containing pyridin-3-ylmethyl 4-(benzoyl)piperazine-1-carbodithioate moiety as potent PKM2 activators

Ridong Li [a,1,*], Xianling Ning [a,1], Jianan He [e], Zhiqiang Lin [a], Yue Su [a], Runtao Li [b,*], Yuxin Yin [a,c,d,*]

[a] Institute of Systems Biomedicine, Beijing Key Laboratory of Tumor Systems Biology, School of Basic Medical Sciences, Peking University Health Science Center, Beijing 100191, PR China
[b] State Key Laboratory of Natural and Biomimetic Drugs, School of Pharmaceutical Sciences, Peking University Health Science Center, Beijing 100191, PR China
[c] Peking-Tsinghua Center for Life Sciences, Peking University Health Science Center, Beijing 100191, PR China
[d] Department of Pathology, School of Basic Medical Sciences, Peking University Health Science Center, Beijing 100191, PR China
[e] Department of Pharmacology and Therapeutics, University of Melbourne, Parkville Victoria 3010, Australia

ARTICLE INFO

Keywords:
PKM2 activator
Sulfonamide
Dithiocarbamate
Nuclear translocation
Anti-tumor activity

ABSTRACT

Pyruvate kinase M2 isoform (PKM2) plays a key role in cancer progression through both metabolic and non-metabolic functions, thus it is recognized as a potential target for cancer diagnosis and treatment. In this study, we discovered a sulfonamide-dithiocarbamate compound **8a** as a novel PKM2 activator from a random screening of an in-house compound library. Then, a series of lead compound **8a** analogs were designed and synthesized for screening as potent PKM2 activators. Among them, compound **8b** (AC_{50} = 0.136 μM) and **8k** (AC_{50} = 0.056 μM) showed higher PKM2 activation activities than positive control **NZT** (AC_{50} = 0.228 μM), and they (IC_{50} < 1 μM) exhibited more significant anti-proliferative activities against human tumor cell lines than **NZT** (IC_{50} > 10 μM). Especially, compound **8k** inhibited the proliferation of multiple cancer cells, but showed little toxicity on normal cells. In addition, we found that compound **8k** inhibit the colony formation of MCF7 cells. Western blot analysis demonstrated that **8k** could reduce PKM2 nuclear localization and block the downstream signaling pathway of PKM2, resulting in suppression of tumor cell proliferation. Overall, compound **8k** may be a promising candidate for further mechanistic investigation of PKM2 and cancer therapy.

1. Introduction

The metabolic pathways of cancer cells distinguish significantly from those of normal cells. Cancer cells produce energy mainly by aerobic glycolysis [1]. Pyruvate kinase (PK) converts phosphoenolpyruvate (PEP) to pyruvate, catalyses the rate limiting step of glycolysis [2,3]. The M1 isoform of pyruvate kinase (PKM1) is found in normal tissues, but the M2 isoform of pyruvate kinase (PKM2), a splicesome variant, is mainly found in cancer cells [4,5]. PKM1 has continuously high enzymatic activity as a stable tetramer. On the contrary, PKM2 exists in balance between less active monomer or dimer and active tetramer form, which can be regulated by some metabolic effectors or post-translational modifications [6-8]. Some allosteric modulators in cancer cells, such as phosphor-tyrosine and post translational modifications, lead to the transformation from PKM2 tetramer to a dimer form. The dimer form diverts the glycolytic flux to biomass production and promotes oncogenesis [9,10]. Moreover, dimer form of PKM2 can translocate into the nucleus to act as a transcriptional activator, even has protein kinase activity [6,11]. For instance, PKM2 phosphorylates STAT3 at Tyr705 resulting in the transcription of downstream genes to promote tumorigenesis [12]. Therefore, switch PKM2 from dimer to tetramer form by small molecule activators may become potent therapeutic strategy [13].

Several PKM2 activators have been reported until now. The representative compounds of PKM2 activators include **TEPP-46** (thieno-[3,2-b]pyrrole[3,2-*d*]pyridazinone) [13,14], **DASA-58** (substituted N,N'-diarylsulfonamide) [13,15], **NZT** (quinoline sulfonamides) [16] and **MCL** (Micheliolide) [17] (Fig. 1). These compounds were reported to

* Corresponding authors at: Institute of Systems Biomedicine, Beijing Key Laboratory of Tumor Systems Biology, School of Basic Medical Sciences, Peking University Health Science Center, Beijing 100191, PR China (Y. Yin).
E-mail addresses: lrd@bjmu.edu.cn, lirt@bjmu.edu.cn (R. Li), yinyuxin@hsc.pku.edu.cn (Y. Yin).
[1] These authors contribute equally to this work.

https://doi.org/10.1016/j.bioorg.2021.104653
Received 1 October 2020; Received in revised form 8 January 2021; Accepted 9 January 2021
Available online 19 January 2021

promote tetramer formation of PKM2, affect the translocation of PKM2 into the nucleus, and inhibit the lysine433 acetylation. Although many PKM2 activators were discovered, most of them have limited effects on cell viability in cell culture using standard conditions [13,18]. Recently, our group has also reported two series of PKM2 activators with different structural types. One kind is 7-azaindole derivative containing pyridin-3-ylmethyl dithiocarbamate moiety (**5** / AC_{50} = 1.00 μM and **6** / AC_{50} = 2.67 μM) [19,20]. Another kind is sulfonamide derivative containing 4-hydroxythiazolidine-2-thione (**7** / AC_{50} = 3.14 μM) [21]. To our delight, our PKM2 activators could effectively inhibit cellular growth on tumor cell lines, while maintaining low toxicities towards non-cancer cell lines.

Combined with literature reports [15,16,22,23] and our previous studies [21], it was found that sulfonamides have good PKM2 activation activity. Furthermore, our previous works have showed that dithiocarbamate moiety is crucial for improving PKM2 potency and selectivity [19,20]. In the past twenty years, our group has been committed to the research of dithiocarbamates as anti-tumor agents [19,20,24-28]. As a continuation of searching new types of PKM2 activators, we conducted a random screening of an in-house dithiocarbamate compound library (~500 total) on the basis of the established PKM2 model. Fortunately, we identified a novel compound **8a** (Fig. 2) with 60.4% activation rate on PKM2 at a concentration of 5 μM. To the best of our knowledge, this type of sulfonamide-dithiocarbamates as PKM2 activator has not been reported before. More interestingly, this novel sulfonamide-dithiocarbamate showed significant anti-tumor activities in the preliminary anti-tumor screening. Especially for cell lines PC3 and A375, the IC_{50} values of **8a** were 3.06 μM and 2.67 μM, respectively. These results demonstrate that compound **8a** is a valuable lead compound for the development of PKM2 activators. Our previous studies [19-21] have showed that the pyridin-3-methylene moiety of compound **8a** is crucial for antitumor activity. Therefore, in order to further improve the activity, we focused our attention on the modification of phenyl of compound **8a**, which was replaced with aryl or heterocyclic rings, as well as aliphatic chains (Fig. 2).

2. Results and discussion

2.1. Chemistry

The synthetic route for designed compounds **8a-8m** is shown in Schemes 1. The 4-nitrobenzoyl chloride **9** served as a starting material reacted with *tert*-butyl piperazine-1-carboxylate in THF to provide the intermediate *tert*-butyl 4-(4-nitrobenzoyl)piperazine-1-carboxylate **10** under the catalysis of triethylamine. The compound **10** was deprotected in the present of 4 M HCl in dioxane and CH_2Cl_2 and got the intermediate **11**. Without further purification, the intermediate **11** reacted with 3-(chloromethyl)pyridine and carbon disulfide using triethylamine as base in DMF to gain pyridin-3-ylmethyl 4-(4-nitrobenzoyl) piperazine-1-carbodithioate **12**. The reduction of **12** using Fe and NH_4Cl as catalysts in H_2O and EtOH generated pyridin-3-ylmethyl 4-(4-aminobenzoyl)piperazine-1-carbodithioate **13**. Then a variety of commercially available substituted sulfonyl chlorides reacted with compound **13** using pyridine as base in the THF and DMF mixed solvents to provide the corresponding target compounds **8a-8m**.

2.2. Biological evaluation

All target compounds were evaluated for the cell-free PKM2 activation activity with a fluorescent PK-LDH coupled assay as previously reported [19]. The reported PKM2 activator **NZT** was used as the positive control. The PKM2 activation rates of all target compounds at a concentration of 5 μM were firstly examined. As shown in Table 1, compound **8b**, **8c**, **8f**, **8h** and **8k** exhibited high PKM2 activation rates with above 100% at 5 μM. Especially, compound **8b** and **8k** showed the most prominent PKM2 activation rates (275.7% and 286.4%). These compounds with high PKM2 activation rates at 5 μM were further evaluated for their AC_{50} values. Among them, compound **8b** and **8k** with AC_{50} values of 0.136 μM and 0.056 μM respectively, displayed more potent activities than the positive control **NZT** (AC_{50} = 0.228 μM). The different structures at region R showed great impact on the PKM2 activation activities. Firstly, when R was a benzene ring, the PKM2 activation rate was 60.4% at 5 μM. Introduction of an ortho- or *meta*-methoxyl on the benzene ring (**8b**, Activation rate at 5 μM = 275.7%; **8c**, Activation rate at 5 μM = 157.1%) increased the activities. On the contrary, *para*-methoxyl on the benzene ring led to a decrease in potency (**8d**, Activation rate at 5 μM = 20.8%). Introduction of fluorine instead of methoxyl on the benzene ring reduced the activation activities. The *meta*-fluoro analog (**8f**) brought about higher activity than the ortho- (**8e**) and *meta*-fluoro analogs (**8g**). Replacing the benzene ring of compound **8a** with naphthalene ring (**8h**, Activation rate at 5 μM = 103.7%) and quinoline ring (**8k**, Activation rate at 5 μM = 286.4%) resulted in significant increase of activities. However, when the benzene ring was replaced by thiophene (**8i**, Activation rate at 5 μM = 40.4%), 2,3-dihydrobenzo[b][1,4]dioxine (**8j**, Activation rate at 5 μM = 21.9%), 1*H*-pyrrolo[2,3-*b*]pyridine (**8l**, Activation rate at 5 μM = 28.3%), ethenyl (**8m**, Activation rate at 5 μM = 27.7%), the activities reduced obviously. Above all, compound **8k** not only exhibited better activity (AC_{50} = 0.056 μM), but also showed the highest activation (286.4%).

To get further insight into the binding profile and reveal the structure–activity relationship of the newly synthesized compounds, a

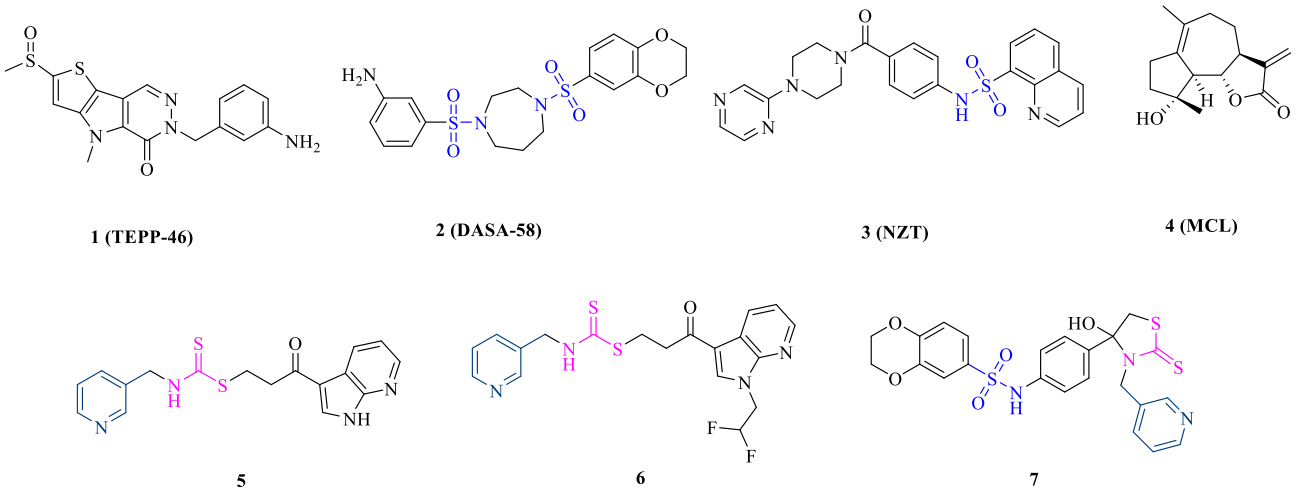

Fig. 1. The structures of representative PKM2 activators.

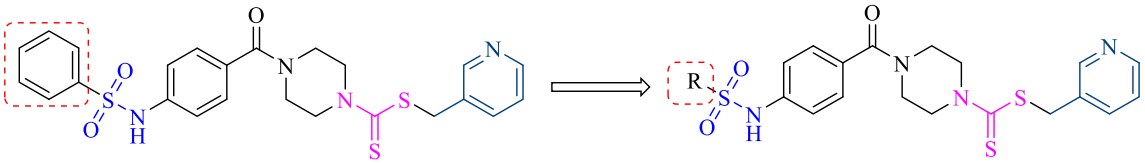

Fig. 2. Lead compound **8a** and overall strategy for its structural modification.

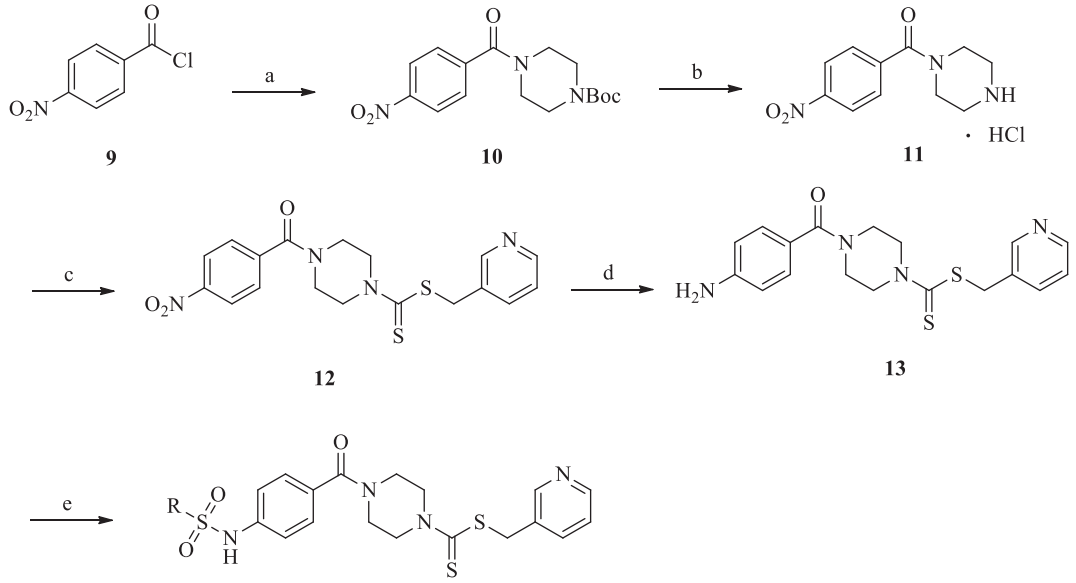

Compd.	R	Compd.	R	Compd.	R
8a		**8f**		**8k**	
8b		**8g**		**8l**	
8c		**8h**		**8m**	
8d		**8i**			
8e		**8j**			

Scheme 1. Synthesis **of 8a-8m**. Reagents and conditions: (a) *tert*-butyl piperazine-1-carboxylate, Et_3N, THF; (b) 4 M HCl in dioxane, CH_2Cl_2; (c) CS_2, 3-(chloromethyl)pyridine hydrochloride, Et_3N, DMF; (d) Fe, NH_4Cl, H_2O, EtOH; (e) THF/DMF 1:1, RSO_2Cl, Pyridine.

docking study of the compound **8k** with PKM2 was carried out. The binding mode of the compound **8k** in the activator pocket of PKM2 is shown in Fig. 3. Our results demonstrate that compound **8k** binds into the pocket with an overall binding affinity of 13.3 kcal/mol, and shares a very similar binding mode with **NZT**. The carbonyl group, sulfonyl group and imino group of the compound are found to be engaged in a hydrogen bonding with the hydrophobic side chain of Lys311B, Tyr390A and Leu353A, respectively. Furthermore, an effective π-π

Table 1
PKM2 activation activities of target compounds **8a-8m**.

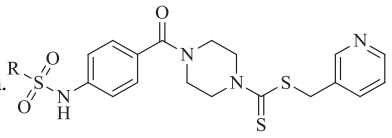

8a-8m

Compd.	R	Activation rate at 5 μM (%)	AC_{50} (μM)[a]
8a		60.4	N.d[b]
8b	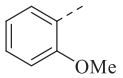	275.7	0.136 ± 0.040
8c	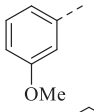	157.1	0.508 ± 0.103
8d	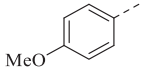	20.8	N.d
8e		57.1	N.d
8f		102.0	0.624 ± 0.157
8g	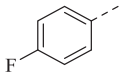	31.5	N.d
8h	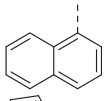	103.7	0.307 ± 0.081
8i		40.4	N.d
8j	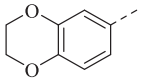	21.9	N.d
8k	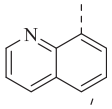	286.4	0.056 ± 0.011
8l	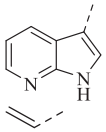	28.3	N.d
8m		27.7	N.d
NZT	—	151.9	0.228 ± 0.062

[a] AC_{50} represents half maximal active concentration.
[b] N.d represents not determined.

stacking interaction was found between the quinolone ring and Phe26B. These interactions are identical to the pattern of binding between the original ligand and the receptor. In addition, a pair of pi-pi stacking interactions are present between the pyridyl group and Phe26B, and also the benzene group and Phe26A. Overall, by analyzing the binding pocket of PKM2 receptor, it was observed that compound **8k** exhibited stronger interaction indicating higher selectivity than PKM2 receptor activator **NZT**. Predictions from the docking results correspond to the bioassay results, making the simulation model reliable and useful for further compound modifications.

To evaluate the potency of target compounds as anti-tumor agents, we measured the effect of target compounds on cancer cells cytotoxicity. The cytotoxicity was assessed using two PKM2 high expression human tumor cell lines derived from human prostate cancer (PC3) and melanoma (A375). Paclitaxel was used as the positive control. The results are shown in Table 2. The IC_{50} values of tested compounds against PC3 and A375 cells ranged between 0.28 and 10 μM. Almost all target compounds showed higher anti-proliferative activities than **NZT**. These results once again demonstrate that our PKM2 activators containing dithiocarbamate moiety have potent antitumor activities. Those compounds with excellent enzymatic activities also have significant anti-proliferative activities. In particular, compound **8b** and **8k** exhibited the optimal activities with IC_{50} values in the nanomolar range, which are also potent at enzyme level. Structure-activity relationship (SAR) analysis showed that introduction of *ortho*-methoxyl on the benzene ring (**8b**) display 3-fold increase in anti-proliferative activities against two cell lines comparing with lead compound **8a**. On the contrary, introduction of *meta*-methoxyl (**8c**) or *para*-fluorine (**8f**) on the benzene ring result in 2-fold or 3-fold decrease in anti-proliferative activities. The different heterocyclic structures at region R also showed great impact on the anti-proliferative activities. When the phenyl group was replaced with thiophene ring (**8i**), 2,3-dihydrobenzo[b][1,4]dioxine (**8j**) or quinoline (**8k**), the corresponding compounds showed slight or significant improvements in comparison with compound **8a**. However, replacement with benzene ring with 7-azaindole (**8l**) resulted in a slight decrease in cellular potency. In addition, replacing the benzene ring of compound **8a** with ethenyl (**8m**) has no significant effect on cell viability.

In additions, compound **8k** and **NZT** were tested in human cervical carcinoma cell (Hela), human breast adenocarcinoma cell (MCF7), human carcinoma cell (CNE2) and human lung cancer cell (A549) to further evaluate anti-proliferative effects by MTS assay. As shown in Table 3, compound **8k** exhibited remarkable inhibitory activities on all the tested tumor cells. In contrast, **NZT** had little inhibitory effects on MCF7 and CNE2 cell lines. In addition, compound **8k** inhibited the colony formation of MCF7 cells in a dose-dependent manner (Fig. 4). To preliminary explore safety of compound **8k**, we tested its cytotoxicity on normal human primary fibroblast cells (BJ cells). The result showed that compound **8k** (IC_{50} > 40 μM) had little toxicity on BJ cells (Table 3), indicating better safety windows.

Previous studies suggested that nuclear PKM2 can function as a protein kinase and transcriptional coactivator to induce the expression of genes, leading to the upregulation of glycolytic gene and promotes tumor development [12]. For example, nuclear PKM2 was found to induce the initiation of STAT3 signaling, which decreased the proportion of apoptotic tumor cells [29]. In addition, PKM2 was also necessary to induce sustained ERK activation and mitogen-induced cell proliferation [30]. To explore whether compound **8k** can influence the nuclear transcription of PKM2, we incubated MCF7 cells with compound **8k** and then separated cytoplasmic and nuclear protein to detect the localization of PKM2. Western blot indicated that nuclear transcription of PKM2 decreased with compound **8k** treatment in a dose-dependent manner (Fig. 5). To demonstrate whether blocking PKM2 nuclear localization could inhibit the expression of PKM2 downstream signaling pathway, we treated cells with compound **8k** and detected the expression of phosphorylated Stat3 and ERK. As shown in Fig. 6, the results showed that the expression of total Stat3 and ERK had not changed obviously, but phosphorylated Stat3 and ERK were significantly inhibited at 5 μM compound **8k**. These results indicated that compound **8k** as a potent PKM2 activator inhibited the PKM2 nuclear translocation in tumor cells, resulting in suppression of transcriptional regulation in tumorigenesis.

3. Conclusion

In this study, the lead compound **8a** was identified as a PKM2 activator from a random screening of an in-house compound library. To explore the SAR and get more potent PKM2 activators, a series of compound **8a** analogs were designed, synthesized and evaluated for their biological activities. Among them, compound **8b** and **8k** showed higher PKM2 activation activities than positive control **NZT**, and also exhibited more significant anti-proliferative activities on human tumor cell lines than **NZT**. In particular, compound **8k** inhibited the

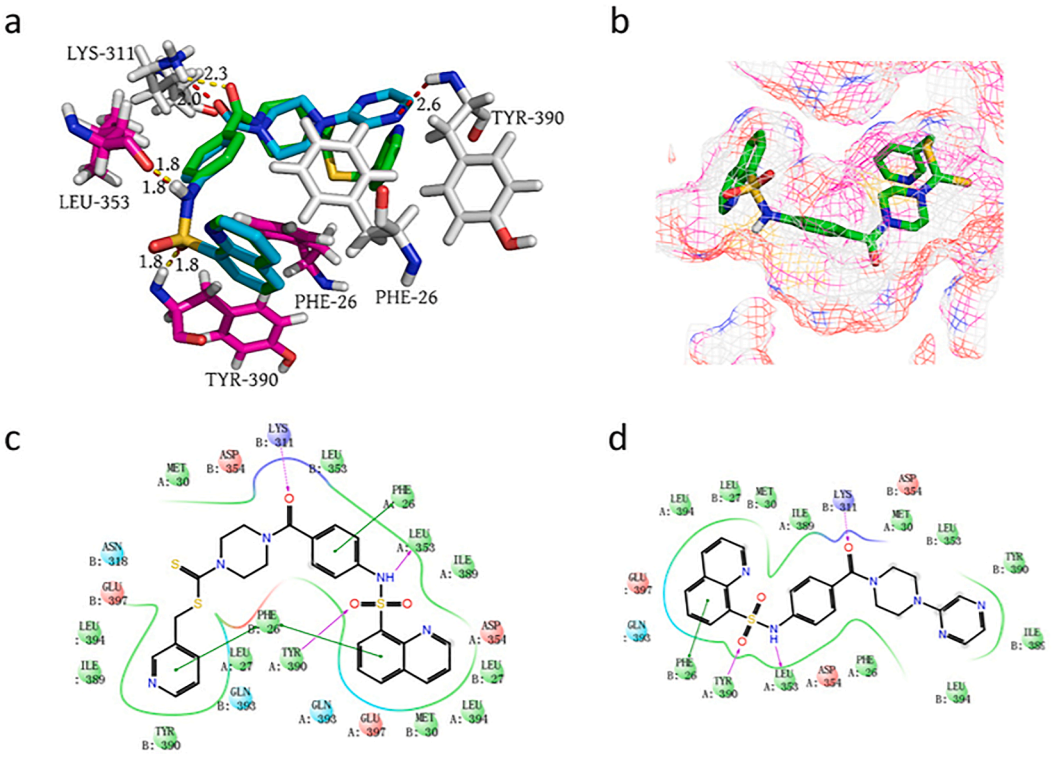

Fig. 3. The predicted docking mode of compound **8k** and PKM2 receptor. a. The predicted 3D binding plot: residues of chain A and chain B of the receptor are colored purple and white, respectively. Yellow dashes indicate hydrogen bonds or polar contacts between compound **8k** and the receptor, and red dashes indicate hydrogen bonds or polar contacts between **NZT** and the receptor, while the number to the next demonstrates the distance of the interaction. Compound **8k** (Green sticks) is aligned with the original ligand (Cyan sticks) from the receptor (PDB ID: 4G1N, ligand: **NZT**) in its crystallized conformation. These two conformations are almost completely coincident. b. Surface plot: Surface (shown as mesh) of residues which are within 12 Å of the compound **8k**. Blue, red and yellow grids represent nitrogen, oxygen and sulfur atoms, respectively. c. The predicted 2D binding mode of compound **8k** to the receptor. d. The predicted 2D binding mode of **NZT** to the receptor. (For interpretation of the references to colour in this figure legend, the reader is referred to the web version of this article.)

proliferation of multiple cancer cells, but showed little toxicity on normal cells, which indicated compound **8k** may have a high safety index. Further mechanistic studies revealed that **8k** could inhibit the colony formation of MCF7 cells, as well as reduce the PKM2 nuclear localization and block the downstream signaling pathways of PKM2, resulting in inhibition of tumor cell proliferation. In summary, these findings reveal that sulfonamide-dithiocarbamate derivatives represent a new class of PKM2 activators that warrant further investigation to generate potential anticancer agents.

4. Experimental section

4.1. General

All reagents and solvents were purchased from commercial sources and were used without further purification. Melting points were determined on X4 microscope and are uncorrected. ^{1}H NMR and ^{13}C NMR spectra were recorded on Bruker AVANCEIII 400 MHz and 100 MHz spectrometer respectively. High resolution mass spectrum (HRMS) was recorded on a Thermo Scientific Orbitrap Elite MS.

4.2. The procedure for the synthesis of tert-butyl 4-(4-nitrobenzoyl) piperazine-1-carboxylate (10)

To a solution of *tert*-butyl piperazine-1-carboxylate (4.66 g, 25 mmol) and triethylamine (6.9 mL, 50 mmol) in THF (40 mL), 4-nitrobenzoyl chloride (4.64 g, 25 mmol) was added slowly. The reaction mixture was stirred at room temperature for 12 h. Water (100 mL) was added and the mixture was extracted with ethyl acetate (20 mL × 3), the combined organic phase was washed with water (30 mL × 2), dried over anhydrous Na_2SO_4 and concentrated under vacuum to afford the crude product. The crude product was purified by column chromatography (eluent: petroleum ether/ethyl acetate = 1:1) to provide compound **10** as light yellow solid (7.70 g, yield: 93%). ^{1}H NMR (400 MHz, DMSO-d_6) δ 8.31 – 8.28 (m, 2H), 7.72 – 7.69 (m, 2H), 3.63 (s, 1H), 3.45 (s, 1H), 3.33 (s, 1H), 3.27 (s, 1H), 1.41 (s, 9H). ^{13}C NMR (100 MHz, DMSO-d_6) δ 167.26, 153.77, 147.81, 142.03, 128.32, 123.74, 79.22, 46.65, 41.39, 27.97.

4.3. The procedure for the synthesis of (4-nitrophenyl)(piperazin-1-yl) methanone hydrochloride(11)

To a solution of compound **10** (1.68 g, 5 mmol) in dichloromethane (20 mL), 4 M HCl in dioxane (5 mL, 20 mmol) was added slowly. The mixture was stirred at room temperature for 2 h. The formed precipitate was filtrated then the precipitate was dried under vacuum to afford the compound **11**, which was used directly without further purification.

4.4. The procedure for the synthesis of pyridin-3-ylmethyl 4-(4-nitrobenzoyl)piperazine-1-carbodithioate(12)

To a solution of compound **11** (1.09 g, 4 mmol) in DMF (20 mL), Et_3N (2.8 mL, 20 mmol) was added. The reaction mixture was stirred for 5 min and CS_2 (0.46 g, 6 mmol) was added, the reaction mixture was stirred continuously for 30 min. 3-(chloromethyl)pyridine hydrochloride (0.66 g, 4 mmol) was added and this mixture was stirred at room temperature for 4 h. Water (50 mL) was added and the mixture was extracted with ethyl acetate (10 mL × 3), the combined organic phase was washed with brine (30 mL × 2), dried over anhydrous Na_2SO_4 and concentrated. The residue was purified by column chromatography

Table 2
The antiproliferative activities of target compounds **8a-8m** against PC3 and A375 cells.

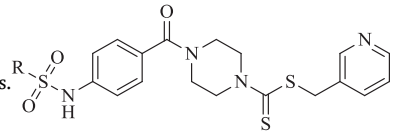

8a–8m

Compd.	R	IC_{50} (μM)[a]	
		PC3	A375
8a		3.06 ± 0.28	2.67 ± 0.28
8b		0.93 ± 0.19	0.85 ± 0.23
8c	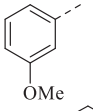	10.01 ± 1.38	9.41 ± 3.48
8d	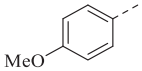	6.60 ± 0.66	3.10 ± 1.83
8e		6.55 ± 1.76	1.98 ± 0.33
8f		4.62 ± 0.58	3.06 ± 0.28
8g	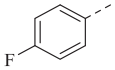	6.36 ± 3.01	7.61 ± 0.83
8h	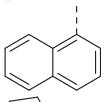	9.44 ± 0.59	6.17 ± 0.39
8i		1.63 ± 0.09	0.83 ± 0.24
8j	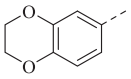	1.86 ± 0.02	0.73 ± 0.01
8k	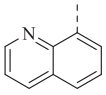	0.97 ± 0.23	0.28 ± 0.02
8l	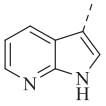	6.39 ± 1.33	5.50 ± 0.35
8m		2.95 ± 0.50	3.34 ± 0.64
NZT	——	> 10	> 10
Paclitaxel	——	0.0046 ± 0.0050	0.0037 ± 0.0012

[a] IC_{50} represents half inhibitory concentration.

Table 3
Anti-proliferative activities of compound **8k** and **NZT** against several tumor cell lines (Hela, MCF7, CNE2 and A549) and non-tumor cell line BJ.

Compd.	IC_{50} (μM)				
	Hela	MCF7	CNE2	A549	BJ
8k	1.23 ± 0.25	0.97 ± 0.13	1.86 ± 0.10	1.47 ± 0.14	>40
NZT	N.d[a]	>50	13.4 ± 0.86	N.d[a]	>40

[a] N.d represents not determined.

(eluent: petroleum ether/ethyl acetate = 3:1) to provide compound **12** as off-white solid solid (1.45 g, yield: 90%). ^{1}H NMR (400 MHz, DMSO-d_6) δ 8.63 (s, 1H), 8.47 (d, J = 4.0 Hz, 1H), 8.32 – 8.29 (m, 2H), 7.81 (d, J = 7.6 Hz, 1H), 7.75 – 7.73 (m, 2H), 7.35 (dd, J = 7.6, 4.8 Hz, 1H), 4.61 (s, 2H), 4.39 – 3.97 (m, 4H), 3.78 (s, 2H), 3.47 (s, 2H). ^{13}C NMR (100 MHz, DMSO-d_6) δ 194.80, 167.38, 150.07, 148.38, 147.93, 141.68, 136.68, 132.65, 128.49, 123.74, 123.47, 45.80, 41.11, 37.44.

*4.5. The procedure for the synthesis of pyridin-3-ylmethyl 4-(4-aminobenzoyl)piperazine-1-carbodithioate(**13**)*

To a solution of compound **12** (1.21 g, 3 mmol) in H_2O (8 mL) and EtOH (24 mL), Fe (0.84 g, 15 mmol) and NH_4Cl (0.23 g, 4.2 mmol) were added. The mixture was heated under reflux for 2 h. The mixture was filtered off and the filtrate was concentrated under vacuum to afford the crude product. The crude product was purified by column chromatography (eluent: petroleum ether/ethyl acetate = 1:1) to provide compound **13** as off- white solid (1.06 g, yield: 94%). ^{1}H NMR (400 MHz, DMSO-d_6) δ 8.62 (s, 1H), 8.47 (d, J = 4.0 Hz, 1H), 7.81 (d, J = 7.6 Hz, 1H), 7.35 (dd, J = 7.6, 4.8 Hz, 1H), 7.18 (d, J = 8.8 Hz, 2H), 6.56 (d, J = 8.4 Hz, 2H), 5.59 (s, 2H), 4.61 (s, 2H), 4.28 (s, 2H), 3.98 (s, 2H), 3.65 – 3.63 (m, 4H). ^{13}C NMR (100 MHz, DMSO-d_6) δ 194.50, 170.05, 150.82, 150.06, 148.35, 136.72, 132.71, 129.50, 123.49, 121.14, 112.62, 50.90, 49.48, 37.42.

*4.6. General procedure for the synthesis of compounds **8a-8m***

To a solution of compound **13** (0.19 g, 0.5 mmol) and pyridine (0.16 mL, 2 mmol) in THF (10 mL) and DMF (5 mL), the substituted sulfonyl chloride (0.5 mmol) was added slowly. The reaction mixture was stirred at room temperature for 12 h. Water (50 mL) was added and the mixture was extracted with ethyl acetate (10 mL × 3), the combined organic phase was washed with 1 N hydrochloric acid (30 mL × 2) and water (30 mL × 2), dried over anhydrous Na_2SO_4 and concentrated under vacuum to afford the crude product. The crude product was purified by column chromatography to provide target products **8a-8m**.

*4.6.1. pyridin-3-ylmethyl 4-(4-(phenylsulfonamido)benzoyl)piperazine-1-carbodithioate (**8a**)*

Yield 74%. ^{1}H NMR (400 MHz, DMSO-d_6) δ 10.64 (s, 1H), 8.61 (s, 1H), 8.46 (dd, J = 4.8, 1.6 Hz, 1H), 7.82 – 7.79 (m, 3H), 7.62 – 7.55 (m, 3H), 7.35 (d, J = 7.2 Hz, 3H), 7.16 (s, 2H), 4.60 (s, 2H), 4.27 (s, 2H), 3.97 (s, 2H), 3.57 (s, 4H). ^{13}C NMR (100 MHz, DMSO-d_6) δ 194.65, 168.72, 150.03, 148.34, 139.44, 139.24, 136.73, 133.10, 132.68, 130.26, 129.37, 128.67, 126.61, 123.46, 118.68, 50.98, 49.83, 37.40. HRMS *m/z*: calcd for $C_{24}H_{25}N_4O_3S_3$ $[M+H]^+$: 513.1089; found: 513.1086.

*4.6.2. pyridin-3-ylmethyl 4-(4-(2-methoxyphenylsulfonamido)benzoyl) piperazine-1- carbodithioate (**8b**)*

Yield 62%. ^{1}H NMR (400 MHz, DMSO-d_6) δ 10.36 (s, 1H), 8.60 (d, J = 2.0 Hz, 1H), 8.46 (dd, J = 4.8, 1.6 Hz, 1H), 7.84 – 7.78 (m, 2H), 7.60 – 7.55 (m, 1H), 7.36 – 7.29 (m, 3H), 7.18 – 7.13 (m, 3H), 7.06 (t, J = 7.6 Hz, 1H), 4.59 (s, 2H), 4.26 (s, 2H), 3.96 (s, 2H), 3.86 (s, 3H), 3.56 (s, 4H). ^{13}C NMR (100 MHz, DMSO-d_6) δ 194.64, 168.79, 156.40, 150.07, 148.38, 139.57, 136.68, 135.23, 132.65, 130.25, 129.68, 128.50, 126.32, 123.45, 120.13, 118.06, 112.98, 56.12, 50.58, 49.12, 37.41. HRMS *m/z*: calcd for $C_{25}H_{27}N_4O_4S_3$ $[M+H]^+$: 543.1194; found: 543.1185.

*4.6.3. pyridin-3-ylmethyl 4-(4-(3-methoxyphenylsulfonamido)benzoyl) piperazine-1- carbodithioate (**8c**)*

Yield 70%. ^{1}H NMR (400 MHz, DMSO-d_6) δ 10.60 (d, J = 2.8 Hz, 1H), 8.61 (s, 1H), 8.46 (dd, J = 4.8, 1.2 Hz, 1H), 7.80 (d, J = 8.0 Hz, 1H), 7.48 (t, J = 8.0 Hz, 1H), 7.37 – 7.29 (m, 5H), 7.20 – 7.16 (m, 3H), 4.60 (s, 2H), 4.27 (s, 2H), 3.95 (s, 2H), 3.77 (s, 3H), 3.59 (s, 4H). ^{13}C NMR (100 MHz, DMSO-d_6) δ 194.67, 168.72, 159.37, 150.06, 148.37, 140.62, 139.21, 136.70, 132.66, 130.60, 130.40, 128.67, 123.45, 118.88, 118.80, 118.68, 111.69, 55.58, 50.69, 49.20, 37.41. HRMS *m/z*: calcd for $C_{25}H_{27}N_4O_4S_3$ $[M+H]^+$: 543.1194; found: 543.1191.

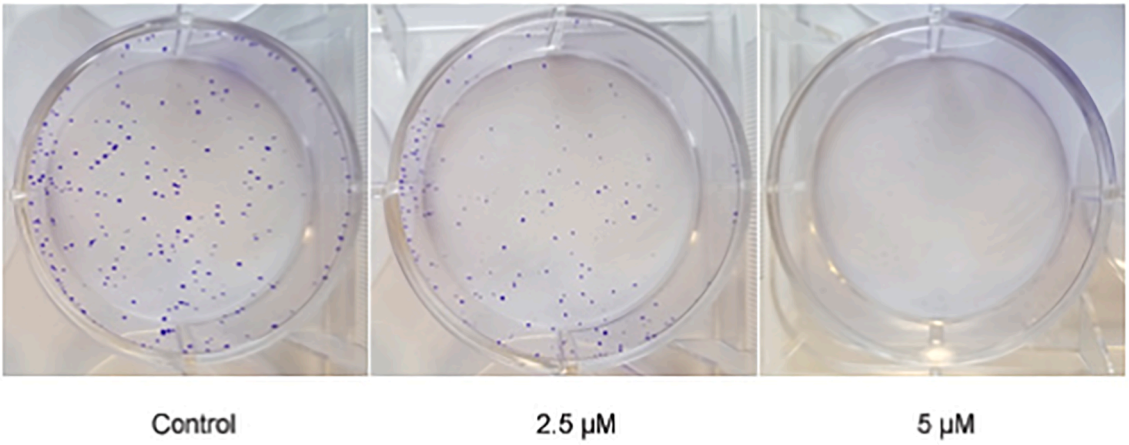

Fig. 4. Compound **8k** inhibited the clone formation of MCF7 cells. MCF7 cells were exposed to 0, 2.5 and 5 μM compound **8k** for 10 days.

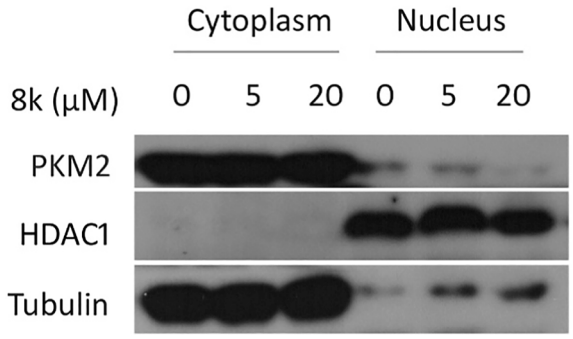

Fig. 5. Compound **8k** reduced the nuclear localization of PKM2. Cells were treated with 0, 5 and 20 μM compound **8k** for 24 h, and the cytoplasmic and nuclear fractions were separated. Tubulin and HDAC1 were used as cytosolic and nuclear loading controls, respectively.

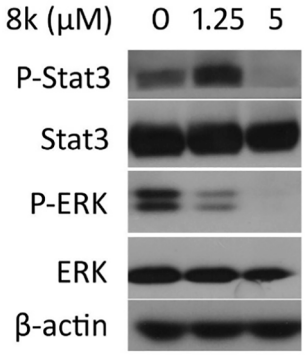

Fig. 6. Compound **8k** down-regulated the downstream pathway of PKM2. Cells were treated with 0, 1.25 and 5 μM compound **8k** for 24 h.

*4.6.4. pyridin-3-ylmethyl 4-(4-(4-methoxyphenylsulfonamido)benzoyl) piperazine-1- carbodithioate (**8d**)*

Yield 66%. ^{1}H NMR (400 MHz, DMSO-d_6) δ 10.48 (s, 1H), 8.60 (d, J = 2.0 Hz, 1H), 8.46 (dd, J = 4.8, 1.6 Hz, 1H), 7.81 – 7.72 (m, 3H), 7.36 – 7.33 (m, 3H), 7.14 (d, J = 8.8 Hz, 2H), 7.07 (d, J = 8.8 Hz, 2H), 4.60 (s, 2H), 4.27 (s, 2H), 3.97 (s, 2H), 3.79 (s, 3H), 3.58 (s, 4H). ^{13}C NMR (100 MHz, DMSO-d_6) δ 194.66, 168.78, 162.56, 150.08, 148.38, 139.50, 136.69, 132.66, 131.01, 130.02, 128.90, 128.66, 123.45, 118.45, 114.49, 55.63, 50.79, 49.44, 37.42. HRMS *m/z*: calcd for $C_{25}H_{27}N_4O_4S_3$ $[M+H]^+$: 543.1194; found: 543.1191.

*4.6.5. pyridin-3-ylmethyl 4-(4-(2-fluorophenylsulfonamido)benzoyl) piperazine-1- carbodithioate (**8e**)*

Yield 60%. ^{1}H NMR (400 MHz, DMSO-d_6) δ 10.97 (s, 1H), 8.60 (d, J = 2.0 Hz, 1H), 8.46 (dd, J = 4.8, 1.6 Hz, 1H), 7.92 – 7.88 (m, 1H), 7.81 – 7.78 (m, 1H), 7.74 – 7.68 (m, 1H), 7.46 – 7.33 (m, 5H), 7.15 (d, J = 8.4 Hz, 1H), 4.59 (s, 2H), 4.26 (s, 2H), 3.96 (s, 2H), 3.57 (s, 4H). ^{13}C NMR (100 MHz, DMSO-d_6) δ 194.66, 168.67, 158.13 (d, J = 253.0 Hz), 150.07, 148.37, 138.75, 136.67, 136.13 (d, J = 9.0 Hz), 132.64, 130.40, 130.31, 128.68, 126.97 (d, J = 14.0 Hz), 125.06 (d, J = 2.0 Hz), 123.43, 118.27, 117.37 (d, J = 20.0 Hz), 50.85, 49.24, 37.41. HRMS *m/z*: calcd for $C_{24}H_{24}FN_4O_3S_3$ $[M+H]^+$: 531.0995; found: 531.0991.

*4.6.6. pyridin-3-ylmethyl 4-(4-(3-fluorophenylsulfonamido)benzoyl) piperazine-1- carbodithioate (**8f**)*

Yield 67%. ^{1}H NMR (400 MHz, DMSO-d_6) δ 10.73 (s, 1H), 8.61 (s, 1H), 8.46 (d, J = 4.8 Hz, 1H), 7.80 (d, J = 7.2 Hz, 1H), 7.65 – 7.62 (m, 3H), 7.51 (d, J = 4.4 Hz, 1H), 7.39 – 7.33 (m, 3H), 7.18 (d, J = 3.2 Hz, 2H), 4.60 (s, 2H), 4.28 (s, 2H), 3.97 (s, 2H), 3.59 (s, 4H). ^{13}C NMR (100 MHz, DMSO-d_6) δ 194.68, 168.68, 161.66 (d, J = 247.0 Hz), 150.08, 148.38, 141.41 (d, J = 6.0 Hz), 138.82, 136.70, 132.66, 131.82, 130.70, 128.74, 123.45, 122.95 (d, J = 3.0 Hz), 120.38 (d, J = 21.0 Hz), 119.12, 113.69 (d, J = 24.0 Hz), 50.68, 49.20, 37.43. HRMS *m/z*: calcd for $C_{24}H_{24}FN_4O_3S_3$ $[M+H]^+$: 531.0995; found: 531.0989.

*4.6.7. pyridin-3-ylmethyl 4-(4-(4-fluorophenylsulfonamido)benzoyl) piperazine-1- carbodithioate (**8g**)*

Yield 64%. ^{1}H NMR (400 MHz, DMSO-d_6) δ 10.63 (s, 1H), 8.60 (d, J = 1.6 Hz, 1H), 8.46 (dd, J = 4.8, 1.6 Hz, 1H), 7.86 (dd, J = 8.8, 5.2 Hz, 2H), 7.80 (d, J = 8.0 Hz, 1H), 7.41 (t, J = 8.8 Hz, 2H), 7.37 – 7.33 (m, 3H), 7.15 (d, J = 8.0 Hz, 2H), 4.60 (s, 2H), 4.27 (s, 2H), 3.97 (s, 2H), 3.58 (s, 4H). ^{13}C NMR (100 MHz, DMSO-d_6) δ 194.66, 168.68, 163.14, 150.06, 148.37, 139.02, 136.69, 135.74, 132.66, 130.51, 129.72 (d, J = 10.0 Hz), 128.69, 123.45, 118.93, 116.61 (d, J = 22.0 Hz), 50.56, 49.48, 37.40 (s). HRMS *m/z*: calcd for $C_{24}H_{24}FN_4O_3S_3$ $[M+H]^+$: 531.0995; found: 531.0992.

*4.6.8. pyridin-3-ylmethyl 4-(4-(naphthalene-1-sulfonamido)benzoyl) piperazine-1- carbodithioate (**8h**)*

Yield 71%. ^{1}H NMR (400 MHz, DMSO-d_6) δ 11.04 (s, 1H), 8.71 (d, J = 8.4 Hz, 1H), 8.59 (d, J = 2.0 Hz, 1H), 8.45 (dd, J = 4.8, 1.6 Hz, 1H), 8.29 (dd, J = 7.4, 1.0 Hz, 1H), 8.24 (d, J = 8.4 Hz, 1H), 8.08 (d, J = 7.6 Hz, 1H), 7.80 – 7.73 (m, 2H), 7.69 – 7.63 (m, 2H), 7.33 (dd, J = 7.8, 4.2 Hz, 1H), 7.27 (d, J = 8.4 Hz, 2H), 7.08 (d, J = 8.8 Hz, 2H), 4.58 (s, 2H), 4.22 (s, 2H), 3.92 (s, 2H), 3.51 (s, 4H). ^{13}C NMR (100 MHz, DMSO-d_6) δ 194.75, 168.88, 150.06, 148.37, 139.13, 136.67, 134.63, 134.21, 133.77, 132.64, 129.94, 129.76, 129.15, 128.65, 128.23, 127.34,

127.03, 124.51, 124.10, 123.44, 117.65, 50.23, 49.49, 37.38. HRMS *m/z*: calcd for $C_{28}H_{27}N_4O_3S_3$ $[M+H]^+$: 563.1245; found: 563.1240.

4.6.9. pyridin-3-ylmethyl 4-(4-(thiophene-2-sulfonamido)benzoyl) piperazine-1- carbodithioate (**8i**)

Yield 65%. ^{1}H NMR (400 MHz, DMSO-d_6) δ 10.75 (s, 1H), 8.61 (d, J = 2.0 Hz, 1H), 8.46 (dd, J = 4.8, 1.6 Hz, 1H), 7.92 (d, J = 4.8 Hz, 1H), 7.80 (d, J = 8.0 Hz, 1H), 7.62 (dd, J = 2.6, 1.0 Hz, 1H), 7.39 (d, J = 8.4 Hz, 2H), 7.34 (dd, J = 7.8, 5.0 Hz, 1H), 7.21 (d, J = 8.0 Hz, 2H), 7.13 (dd, J = 4.8, 4.0 Hz, 1H), 4.60 (s, 2H), 4.28 (s, 2H), 3.98 (s, 2H), 3.60 (s, 4H). ^{13}C NMR (100 MHz, DMSO-d_6) δ 194.66, 168.72, 150.06, 148.37, 139.82, 138.96, 136.71, 134.32, 133.63, 132.68, 130.63, 128.65, 127.70, 123.46, 119.02, 50.51, 49.07, 37.41. HRMS *m/z*: calcd for $C_{22}H_{23}N_4O_3S_4$ $[M+H]^+$: 519.0653; found: 519.0642.

4.6.10. pyridin-3-ylmethyl 4-(4-(2,3-dihydrobenzo[b][1,4]dioxine-6-sulfonamido) benzoyl)piperazine-1-carbodithioate (**8j**)

Yield 63%. ^{1}H NMR (400 MHz, DMSO-d_6) δ 10.71 (s, 1H), 8.61 (s, 1H), 8.46 (d, J = 4.0 Hz, 1H), 7.80 (d, J = 8.0 Hz, 1H), 7.36 – 7.28 (m, 5H), 7.20 (d, J = 8.8 Hz, 2H), 7.00 (d, J = 8.4 Hz, 1H), 4.60 (s, 2H), 4.28 (dd, J = 8.6, 4.6 Hz, 6H), 3.98 (s, 2H), 3.59 (s, 4H). ^{13}C NMR (100 MHz, DMSO-d_6) δ 194.65, 168.80, 150.05, 148.36, 147.29, 143.26, 139.52, 136.70, 132.68, 131.85, 130.02, 128.60, 123.47, 120.33, 118.50, 117.61, 115.65, 64.33, 64.02, 50.82, 49.43, 37.40. HRMS *m/z*: calcd for $C_{26}H_{27}N_4O_5S_3$ $[M+H]^+$: 571.1144; found: 571.1130.

4.6.11. pyridin-3-ylmethyl 4-(4-(quinoline-8-sulfonamido)benzoyl) piperazine-1- carbodithioate (**8k**)

Yield 58%. ^{1}H NMR (400 MHz, DMSO-d_6) δ 10.49 (s, 1H), 9.13 (dd, J = 4.4, 1.6 Hz, 1H), 8.59 (d, J = 2.0 Hz, 1H), 8.51 (dd, J = 8.0, 1.2 Hz, 1H), 8.46 – 8.43 (m, 2H), 8.29 (d, J = 7.6 Hz, 1H), 7.80 – 7.70 (m, 3H), 7.33 (dd, J = 7.6, 4.8 Hz, 1H), 7.22 (d, J = 8.4 Hz, 2H), 7.13 (d, J = 8.4 Hz, 2H), 4.58 (s, 2H), 4.22 (s, 2H), 3.92 (s, 2H), 3.51 (s, 4H). ^{13}C NMR (100 MHz, DMSO-d_6) δ 194.63, 168.72, 151.47, 150.06, 148.36, 142.70, 139.47, 136.97, 136.65, 135.17, 134.41, 132.63, 132.23, 129.76, 128.40, 125.62, 123.42, 122.63, 118.33, 50.62, 49.08, 37.42. HRMS *m/z*: calcd for $C_{27}H_{26}N_5O_3S_3$ $[M+H]^+$: 564.1198; found: 564.1185.

4.6.12. pyridin-3-ylmethyl 4-(4-(1H-pyrrolo[2,3-b]pyridine-3-sulfonamido)benzoyl) piperazine-1-carbodithioate (**8l**)

Yield 57%. ^{1}H NMR (400 MHz, DMSO-d_6) δ 12.65 (s, 1H), 10.55 (s, 1H), 8.60 (d, J = 2.0 Hz, 1H), 8.45 (dd, J = 4.6, 1.4 Hz, 1H), 8.34 (dd, J = 4.8, 1.6 Hz, 1H), 8.21 (s, 1H), 8.18 (d, J = 8.0 Hz, 1H), 7.79 (d, J = 8.0 Hz, 1H), 7.35 – 7.24 (m, 4H), 7.17 – 7.15 (m, 2H), 4.59 (s, 2H), 4.24 (s, 2H), 3.94 (s, 2H), 3.56 (s, 4H). ^{13}C NMR (100 MHz, DMSO-d_6) δ 194.63, 168.79, 150.06, 148.37, 147.96, 144.67, 139.69, 136.69, 132.66, 131.80, 129.56, 128.55, 127.47, 123.45, 117.88, 117.61, 115.48, 111.84, 50.52, 49.99, 37.39. HRMS *m/z*: calcd for $C_{25}H_{25}N_6O_3S_3$ $[M+H]^+$: 553.1150; found: 553.1146.

4.6.13. pyridin-3-ylmethyl 4-(4-(vinylsulfonamido)benzoyl)piperazine-1-carbodithioate (**8m**)

Yield 42%. ^{1}H NMR (400 MHz, DMSO-d_6) δ 10.35 (s, 1H), 8.61 (d, J = 2.0 Hz, 1H), 8.46 (dd, J = 4.8, 1.6 Hz, 1H), 7.81 (d, J = 8.0 Hz, 1H), 7.41 (d, J = 8.4 Hz, 2H), 7.35 (dd, J = 7.6, 4.8 Hz, 1H), 7.18 (d, J = 8.8 Hz, 2H), 6.87 – 6.81 (m, 1H), 6.18 (d, J = 16.4 Hz, 1H), 6.07 (d, J = 10.0 Hz, 1H), 4.60 (s, 2H), 4.29 (s, 2H), 3.99 (s, 2H), 3.63 (s, 4H). ^{13}C NMR (100 MHz, DMSO-d_6) δ 194.69, 168.89, 150.09, 148.40, 139.61, 136.71, 136.26, 132.68, 129.86, 128.70, 127.96, 123.47, 118.34, 50.79, 49.15, 37.45. HRMS *m/z*: calcd for $C_{20}H_{23}N_4O_3S_3$ $[M+H]^+$: 463.0932; found: 463.0929.

4.7. PKM2 activity assay

Pyruvate kinase activity was detected with a fluorescent pyruvate kinase-lactate dehydrogenase coupled assay as previously described [19].

4.8. Anti-proliferation activity assay

Cell lines (PC3, A375, Hela, MCF7, CNE2, A549 and BJ) were cultured in DMEM containing 9% fetal bovine serum (FBS) at 37 °C in 5% CO_2. Cell viability was detected with the MTS assay (Promega) according to the manufacturer's instructions. Briefly, 3000–5000 cells in per well were plated in 96-well plates. After incubated for 12 h, the cells were treated with different concentrations of tested compounds or DMSO (as negative control) for 48 h. Then 20 μL MTS was added in per well and incubated at 37 °C for 3 h. Absorbance of each well was determined by a microplate reader (Flexstation 3) at a 490 nm wave length. The IC_{50} values were calculated using Prism Graphpad software of the triplicate experiment.

4.9. Procedures for molecular docking

Molecular docking was carried out by using Open-Source Autodockvina (Scripps Research Institute), pre-processed by Schrodinger Maestro (Peking University) and AutoDock Tools 1.5.6 rc3, assessed by Schrodinger Maestro and Open-Source PyMOL 1.3.x (Schrodinger, LLC) afterwards. The X-ray crystal structure of PKM2 and its reported activator NZT taken from PDB (4G1N) was obtained from protein data bank (https://www.rcsb.org) and used as the input structure. Receptor preparation: All solvent molecules or any other heteromolecules are removed. All HETATM and hydrogen atoms are deleted and crystal cell is removed. Alternative conformers of residues are also deleted to retain one set. The receptor is further processed via AutoDock Tools 1.5.6 rc3. Polar hydrogen and Kollman charge is added to finally give the prepared protein. Ligand preparation: Polar hydrogen and Gasteiger charge is given and there is no further modification on the ligand torsion tree. Molecular docking: Parameter selection is done via AutoDock Tools 1.5.6 rc3. All the remaining parameters were kept as default.

4.10. Colony formation assay

To test the clonogenic capacity of cells in vitro, 600 cells (MCF7) were plated in six-well culture plates. After 24 h incubation, cells were treated with 0, 2.5 and 5 μM compound **8k** for 24 h. Then the medium was changed into fresh medium without compound **8k** and the cells continued to grow for 10 days to form colonies, and then fixed with methanol and stained with crystal violet.

4.11. The separation of cytoplasmic and nuclear protein

MCF7 cells were treated with 0, 5 and 20 μM compound **8k** for 24 h, and cells were harvested and rinsed with PBS. Cells were suspended in 5 volumes of cold Buffer A (10 mM HEPES pH = 7.9, 0.1 mM EDTA, 0.1 mM EGTA, 10 mM KCl, protease inhibitor cocktail, 1 mM DTT, 0.15% NP-40), and allowed to swell on ice for 15 min, the homogenate was centrifuged for 1 min at 12,000*g*. The supernatant containing the cytoplasm fraction was transferred to a fresh tube. The crude nuclear fraction was suspended in buffer B (10 mM Tris pH = 7.9, 1.5 mM $MgCl_2$, 10 mM KCl, 400 mM NaCl, 0.4% Triton X-100 and protease inhibitor cocktail), and vortexed at 4 °C for 30 min. The homogenate was centrifuged for 15 min at 12,000*g*, and the nuclear extract was transferred to a fresh tube.

4.12. Western blot

After cells were treated with compound **8k**, western blotting was performed according to the standard protocol. The Stat3, phospho-Stat3 (Tyr 705), Erk, phospho-Erkand PKM2 antibodies were purchased from Cell Signaling Technology. β-Actin antibody was purchased from MBL. HDAC1 was purchased from Santa Cruz biotechnology. Tubulin was purchased from TransGen Biotech.

Declaration of Competing Interest

The authors declare that they have no known competing financial interests or personal relationships that could have appeared to influence the work reported in this paper.

Acknowledgement

This work was supported by National Natural Science Foundation of China (No.81502905, 81402777).

Appendix A. Supplementary data

Supplementary data to this article can be found online at https://doi.org/10.1016/j.bioorg.2021.104653.

References

[1] Z. Wu, J. Wu, Q. Zhao, S. Fu, J. Jin, Emerging roles of aerobic glycolysis in breast cancer, Clin. Transl. Oncol. 22 (2020) 631–646.
[2] N. Schormann, K.L. Hayden, P. Lee, S. Banerjee, D. Chattopadhyay, An overview of structure, function, and regulation of pyruvate kinases, Protein Sci. 28 (2019) 1771–1784.
[3] M. Alquraishi, D.L. Puckett, D.S. Alani, A.S. Humidat, V.D. Frankel, D.R. Donohoe, J. Whelan, A. Bettaieb, Pyruvate kinase M2: A simple molecule with complex functions, Free Radic. Biol. Med. 1 (2019) 176–192.
[4] K. Zahra, T. Dey, SP.M. Ashish, U. Pandey, Pyruvate Kinase M2 and Cancer: The Role of PKM2 in Promoting Tumorigenesis, Front, Oncol. 2 (2020) 159.
[5] Q. Su, S. Luo, Q. Tan, J. Deng, S. Zhou, M. Peng, T. Tao, X. Yang, The role of pyruvate kinase M2 in anticancer therapeutic treatments, Oncol. Lett. 18 (2019) 5663–5672.
[6] M.C. Hsu, W.C. Hung, Pyruvate kinase M2 fuels multiple aspects of cancer cells: from cellular metabolism, transcriptional regulation to extracellular signaling, Mol. Cancer. 17 (2018) 35.
[7] K.E. Keller, I.S. Tan, Y.S. Lee, SAICAR stimulates pyruvate kinase isoform M2 and promotes cancer cell survival in glucose-limited conditions, Science. 338 (2012) 1069–1072.
[8] W.J. Israelsen, T.L. Dayton, S.M. Davidson, B.P. Fiske, A.M. Hosios, G. Bellinger, J. Li, Y. Yu, M. Sasaki, J.W. Horner, L.N. Burga, J. Xie, M.J. Jurczak, R.A. DePinho, C.B. Clish, T. Jacks, R.G. Kibbey, G.M. Wulf, D. Di Vizio, G.B. Mills, L.C. Cantley, M. G. Vander Heiden, PKM2 isoform-specific deletion reveals a differential requirement for pyruvate kinase in tumor cells, Cell. 155 (2013) 397–409.
[9] T.L. Dayton, T. Jacks, M.G. Vander Heiden, PKM2, cancer metabolism, and the road ahead, EMBO Rep. 17 (2016) 1721–1730.
[10] D.Y. Gui, C.A. Lewis, M.G. Vander Heiden, Allosteric regulation of PKM2 allows cellular adaptation to different physiological states, Sci. signal. 6 (2013) pe7.
[11] X. Gao, H. Wang, J.J. Yang, X. Liu, Z.R. Liu, Pyruvate kinase M2 regulates gene transcription by acting as a protein kinase, Mol. Cell. 45 (2012) 598–609.
[12] Y.H. Li, X.F. Li, J.T. Liu, H. Wang, L.L. Fan, J. Li, G.P. Sun, PKM2, a potential target for regulating cancer, Gene. 668 (2018) 48–53.
[13] D. Anastasiou, Y. Yu, W.J. Israelsen, J.K. Jiang, M.B. Boxer, B.S. Hong, W. Tempel, S. Dimov, M. Shen, A. Jha, H. Yang, K.R. Mattaini, C.M. Metallo, B.P. Fiske, K. D. Courtney, S. Malstrom, T.M. Khan, C. Kung, A.P. Skoumbourdis, H. Veith, N. Southall, M.J. Walsh, K.R. Brimacombe, W. Leister, S.Y. Lunt, Z.R. Johnson, K. E. Yen, K. Kunii, S.M. Davidson, H.R. Christofk, C.P. Austin, J. Inglese, M.H. Harris, J.M. Asara, G. Stephanopoulos, F.G. Salituro, S. Jin, L. Dang, D.S. Auld, H.W. Park, L.C. Cantley, C.J. Thomas, M.G. Vander Heiden, Pyruvate kinase M2 activators promote tetramer formation and suppress tumorigenesis, Nat. Chem. Biol. 8 (2012) 839–847.
[14] J.K. Jiang, M.B. Boxer, M.G. Vander Heiden, M. Shen, A.P. Skoumbourdis, N. Southall, H. Veith, W. Leister, C.P. Austin, H.W. Park, J. Inglese, L.C. Cantley, D. S. Auld, C.J. Thomas, Evaluation of thieno[3,2-b]pyrrole[3,2-d]pyridazinones as activators of the tumor cell specific M2 isoform of pyruvate kinase, Bioorg. Med. Chem. Lett. 20 (2010) 3387–3393.
[15] M.B. Boxer, J.K. Jiang, M.G. Vander Heiden, M. Shen, A.P. Skoumbourdis, N. Southall, H. Veith, W. Leister, C.P. Austin, H.W. Park, J. Inglese, L.C. Cantley, D. S. Auld, C.J. Thomas, Evaluation of substituted N, N'-diarylsulfonamides as activators of the tumor cell specific M2 isoform of pyruvate kinase, J. Med. Chem. 53 (2010) 1048–1055.
[16] C. Kung, J. Hixon, S. Choe, K. Marks, S. Gross, E. Murphy, B. DeLaBarre, G. Cianchetta, S. Sethumadhavan, X. Wang, S. Yan, Y. Gao, C. Fang, W. Wei, F. Jiang, S. Wang, K. Qian, J. Saunders, E. Driggers, H.K. Woo, K. Kunii, S. Murray, H. Yang, K. Yen, W. Liu, L.C. Cantley, M.G. Vander Heiden, S.M. Su, S. Jin, F. G. Salituro, L. Dang, Small molecule activation of PKM2 in cancer cells induces serine auxotrophy, Chem. Biol. 19 (2012) 1187–1198.
[17] J. Li, S. Li, J. Guo, Q. Li, J. Long, C. Ma, Y. Ding, C. Yan, L. Li, Z. Wu, H. Zhu, K. K. Li, L. Wen, Q. Zhang, Q. Xue, C. Zhao, N. Liu, I. Ivanov, M. Luo, R. Xi, H. Long, P. G. Wang, Y. Chen, Natural Product Micheliolide (MCL) Irreversibly Activates Pyruvate Kinase M2 and Suppresses Leukemia, J. Med. Chem. 61 (2018) 4155–4164.
[18] D.J. Kim, Y.S. Park, N.D. Kim, S.H. Min, Y.M. You, Y. Jung, H. Koo, H. Noh, J. A. Kim, K.C. Park, Y.I. Yeom, A novel pyruvate kinase M2 activator compound that suppresses lung cancer cell viability under hypoxia, Mol. Cells. 38 (2015) 373–379.
[19] Y. Zhang, B. Liu, X. Wu, R. Li, X. Ning, Y. Liu, Z. Liu, Z. Ge, Y. Yin, New pyridin-3-ylmethyl carbamodithioic esters activate pyruvate kinase M2 and potential anticancer lead compounds, Bioorg. Med. Chem. 23 (2015) 4815–4823.
[20] B. Liu, X. Yuan, B. Xu, H. Zhang, R. Li, X. Wang, Z. Ge, R. Li, Y. Yin, Synthesis of novel 7-azaindole derivatives containing pyridin-3-ylmethyl dithiocarbamate moiety as potent PKM2 activators and PKM2 nucleus translocation inhibitors, Eur. J. Med. Chem. 170 (2019) 1–15.
[21] R. Li, X. Ning, S. Zhou, Z. Lin, X. Wu, H. Chen, X. Bai, X. Wang, Z. Ge, R. Li, Y. Yin, Discovery and structure-activity relationship of novel 4-hydroxy-thiazolidine-2-thione derivatives as tumor cell specific pyruvate kinase M2 activators, Eur. J. Med. Chem. 143 (2018) 48–65.
[22] M.J. Walsh, K.R. Brimacombe, H. Veith, J.M. Bougie, T. Daniel, W. Leister, L. C. Cantley, W.J. Israelsen, M.G. Vander Heiden, M. Shen, D.S. Auld, C.J. Thomas, M.B. Boxer, 2-Oxo-N-aryl-1,2,3,4-tetrahydroquinoline-6-sulfonamides as activators of the tumor cell specific M2 isoform of pyruvate kinase, Bioorg. Med. Chem. Lett. 21 (2011) 6322–6327.
[23] A. Yacovan, R. Ozeri, T. Kehat, S. Mirilashvili, D. Sherman, A. Aizikovich, A. Shitrit, E. Ben-Zeev, N. Schutz, O. Bohana-Kashtan, A. Konson, V. Behar, O. M. Becker, 1-(sulfonyl)-5-(arylsulfonyl)indoline as activators of the tumor cell specific M2 isoform of pyruvate kinase, Bioorg. Med. Chem. Lett. 22 (2012) 6460–6468.
[24] X. Hou, Z. Ge, T. Wang, W. Guo, J. Cui, T. Cheng, C. Lai, R. Li, Dithiocarbamic acid esters as anticancer agent. Part 1: 4-Substituted-piperazine-1-carbodithioic acid 3-cyano-3,3-diphenyl-propyl esters, Bioorg. Med. Chem. Lett. 16 (2006) 4214–4219.
[25] R. Li, X. Zhang, Q. Li, Z. Ge, R. Li, Novel EGFR inhibitors prepared by combination of dithiocarbamic acid esters and 4-anilinoquinazolines, Bioorg. Med. Chem. Lett. 21 (2011) 3637–3640.
[26] X. Zhang, R. Li, K. Qiao, Z. Ge, L. Zhang, T. Cheng, R. Li, Novel dithiocarbamic acid esters derived from 6-aminomethyl-4-anilinoquinazolines and 6-aminomethyl-4-anilino-3-cyanoquinolines as potent EGFR inhibitors, Arch. Pharm. Chem. Life Sci. 346 (2013) 44–52.
[27] R. Li, H. Wang, Y. Li, Z. Wang, X. Wang, Y. Wang, Z. Ge, R. Li, Discovery and optimization of novel dual dithiocarbamates as potent anticancer agents, Eur. J. Med. Chem. 93 (2015) 381–391.
[28] Y. Wang, R. Li, H. Zhang, Z. Zhang, X. Wang, Z. Ge, R. Li, Structure-activity relationships of novel dithiocarbamates containing α, β-unsaturated ketone fragment as potent anticancer agents, Med. Chem. Res. 28 (2019) 1027–1038.
[29] Q. Li, D. Zhang, X. Chen, L. He, T. Li, X. Xu, M. Li, Nuclear PKM2 contributes to gefitinib resistance via upregulation of STAT3 activation in colorectal cancer, Sci. Rep. 5 (2015) 16082.
[30] W. Yang, Y. Zheng, Y. Xia, H. Ji, X. Chen, F. Guo, C.A. Lyssiotis, K. Aldape, L. C. Cantley, Z. Lu, ERK1/2-dependent phosphorylation and nuclear translocation of PKM2 promotes the Warburg effect, Nat. cell biol. 14 (2012) 1295–1304.